

1 Chemical composition and characteristics of ambient aerosols and rainwater

2 residues during Indian summer monsoon: Insight from aerosol mass

3 spectrometry

4 Authors:

5 Abhishek Chakraborty, Department of Civil Engineering, Indian Institute of Technology Kanpur,
6 Uttar Pradesh, India-208016

7 Tarun Gupta, Department of Civil Engineering and Center for Environmental Science and
8 Engineering, Indian Institute of Technology Kanpur, Uttar Pradesh, India-208016

9 Sachchida N Tripathi, Department of Civil Engineering and Center for Environmental Science
10 and Engineering, Indian Institute of Technology Kanpur, Uttar Pradesh, India-208016

¹¹ Corresponding Authors: Dr. Tarun Gupta, tarun@iitk.ac.in; Dr. S.N.Tripathi, snt@iitk.ac.in

12
13 **Abstract:** Real time composition of non-refractory submicron aerosol (NR-PM₁) is measured via
14 Aerosol mass spectrometer (AMS) for the first time during Indian summer monsoon at Kanpur, a
15 polluted urban location located at the heart of Indo Gangetic Plain (IGP). Submicron aerosols are
16 found to be dominated by organics followed by nitrate. Source apportionment of organic aerosols
17 (OA) via positive matrix factorization (PMF) revealed several types of secondary/oxidized and
18 primary organic aerosols. On average, OA are completely dominated by oxidized OA with a very
19 little contribution from biomass burning OA. During rain events, PM₁ concentration is decreased
20 almost by 60%, but its composition remains nearly the same. Oxidized OA showed slightly more
21 decrease than primary OAs, probably due to their higher hygroscopicity. The presence of organo

22 nitrates (ON) is also detected in ambient aerosols. Apart from real-time sampling, collected fog
23 and rainwater samples were also analyzed via AMS in offline mode and in the ICP-OES
24 (Inductively coupled plasma – Optical emission spectrometry) for elements. The presence of sea
25 salt, organo nitrates and sulfates has been observed. Rainwater residues are also dominated by
26 organics but their O/C ratios are 15-20% lower than the observed values for ambient OA. Alkali
27 metals such as Ca, Na, K are found to be most abundant in the rainwater followed by Zn.
28 Rainwater residues are also found to be much less oxidized than the aerosols present inside the
29 fog water, indicating presence of less oxidized organics. These findings indicate that rain can act
30 as an effective scavenger of different types of pollutants even for submicron particle range.
31 Rainwater residues also contain organo sulfates which indicate that some portion of the dissolved
32 aerosols has undergone aqueous processing, possibly inside the cloud. Highly oxidized and
33 possibly hygroscopic OA during monsoon period compared to other seasons (winter, post
34 monsoon), indicates that they can act more efficiently as cloud condensation nuclei.

35 **Keywords:** Organic aerosols (OA), O/C ratio, rainwater, monsoon, elemental composition

36 **1. Introduction:**

37 Submicron aerosols constitute a large part of the ambient aerosols and can directly absorb/scatter
38 incoming solar radiation depending upon their composition (Cahill et al., 2008; Carslaw et al.,
39 2013) or indirectly reflect the solar radiation by forming cloud droplets while acting as cloud
40 condensation nuclei (CCN). Due to their smaller sizes, they can also penetrate deep into the
41 human respiratory system and cause several respiratory diseases (Dockery and Pope, 1994;
42 Norris et al., 2000). However, depending upon location and season of the year, their properties
43 can vary greatly; hence it is important to characterize submicron aerosols under different
44 atmospheric conditions. Present study location of Kanpur is situated at the heart of Indo Gangetic

45 Plain (IGP) and is home to 4.5 million people (GOI, 2011). Kanpur is a major industrial hub of
46 Northern India and considered to be one of the most polluted city in India and World (National
47 ambient air quality standards, 2012). Mostly unregulated industrial emissions, biomass burning
48 and vehicular emissions are the major sources of particulate pollution at this location (Behera
49 and Sharma, 2010a, 2010b; Kaul et al., 2011).

50 Nearly 60% of the world population depends on the Asian summer monsoon to bring sufficient
51 water for irrigation, drinking water supply and other essential purposes (Hyvarinen et al., 2011).
52 In recent years, several studies have indicated possible effects of pollution on the Summer
53 Monsoon. This may be especially important in Southern Asia since the area suffers from an
54 intense and persistent particulate pollution called the “brown cloud” (Lelieveld et al., 2001;
55 Nakajima et al., 2007; Ramanathan et al., 2007). Hyvärinen et al., (2011) reported 50-70%
56 reduction in $PM_{2.5}$ and PM_{10} concentrations from pre monsoon to monsoon period at a site in the
57 Northern India, however without any detail chemical characterization of $PM_{2.5}$ and PM_{10} . Yadav
58 et al., (2013) characterized non-polar organic compounds of PM_{10} in Delhi during monsoon and
59 reported highest fractional contributions from n-alkanes and BC to PM_{10} due to their
60 hydrophobic nature, which prevented their washout by rain. Several online and offline based
61 aerosol characterization studies have been carried out at this study location as well (Chakraborty
62 and Gupta, 2010; Chakraborty et al., 2015; Kaul et al., 2011; Mishra et al., 2008; Misra et al.,
63 2014), but mostly during winter or summer. Therefore, comprehensive chemical characterization
64 of monsoon time submicron aerosols is yet to be carried out in India, especially types of organic
65 aerosols (OA) present, their contributions and characteristics has never been reported. In this
66 study, with the help of HR-ToF-AMS, we are reporting for the first time what is the composition
67 of OA, what are the different types of OA dominated during monsoon period and how their

68 oxidation ratios (O/C) evolved apart from changes in different inorganic species like sulfate,
69 nitrate, etc.

70 In addition to real time aerosol data, we have also collected and analyzed rainwater samples to
71 understand its composition and what kind of species it is scavenging from the ambient air more
72 efficiently. Several rainwater characterization studies have been carried out in India. Kulshrestha
73 et al., (2005) in a review article on India's precipitation chemistry, compiled results from 100
74 sites with very different characteristics and found that majority of them only measured ions and
75 elements present in the rainwater. Very few characterization study of rainwater organics has been
76 carried out in India. Malik et al., (2007) showed the presence of chlorinated pesticides and PAHs
77 in the rainwater samples collected from Lucknow. Salve et al., (2012) reported the presence of
78 chromophoric organic compounds in rainwater samples collected at Rameswaram. A few studies
79 have also reported the presence of organic acids and acetates in rainwater from India (Khare et
80 al., 1998, 1997; Kulshreshta et al., 1993). However, bulk characteristics of rainwater organics or
81 their overall oxidation levels have never been analyzed. It is interesting to analyze whether OA
82 present inside rainwater are any different from ambient and/or fog water aerosols due to cloud
83 processing and different scavenging efficiencies for different types of ambient OA as reported
84 for fog (Chakraborty et al., 2015; Gilardoni et al., 2014). A real time study of aerosol
85 composition along with OA source apportionment and offline analysis of rainwater in AMS has
86 provided some new insights into the ambient aerosol characteristics during monsoon time.

87 **2. Materials and methods:**

88 Real time, non refractory ambient submicron aerosol sampling (will be referred to as **AA**, from
89 now onwards) was carried out using HR-ToF-AMS from 24 May – 15 Aug 2015. Average

90 meteorological parameters are shown in Table 1. AMS was operated in V mode with 2 min
91 resolution and regular IE calibration was performed using pure NH_4NO_3 solution.

Parameters	Monsoon
RH (%)	69
T (°C)	29.88
WS (m/s)	3.74
PBLH (m)	1024
Rainfall (mm)	466

92

93 Table 1: Average meteorological parameters during monsoon season. PBLH = Planetary
94 boundary layer height.

95 Apart from NH_4NO_3 , pure $(\text{NH}_4)_2\text{SO}_4$ and KNO_3 were also analyzed in AMS to determine ratios
96 of different sulfate and nitrate fragments in the AMS like $\text{SO}^+/\text{SO}_3^+$, $\text{SO}_2^+/\text{SO}_3^+$, $\text{NO}^+/\text{NO}_2^+$ etc.
97 to qualitatively identify any contributions from organic sulfates and/or metallic nitrates. A silica
98 gel drier was placed in front of the AMS to prevent moisture from entering into the sampling
99 lines. Periodical High efficiency particulate attainment (HEPA) filter measurements were taken
100 to assess and rectify the gaseous interference on AMS mass spectra. Based on these
101 measurements, some modifications are made at m/z 18, 28 & 44 of AMS fragmentation table.
102 AMS data analysis is carried in Igor Pro using SQUIRREL 1.51H & PIKA 1.15H AMS data
103 analysis software packages. HR Fitting in V mode is carried out till m/z 150 and accounts for
104 99% of the total AMS measured aerosol mass. A collection efficiency (CE) value of 0.5 is
105 applied to AMS dataset to calculate accurately mass concentrations. This CE is chosen after

106 applying Middlebrook et al., (2012) equation which incorporates aerosol chemical composition,
107 acidity, and RH of sampling line. This value of CE is previously found to be appropriate for most
108 of the locations across the globe including for this location (Bhattu and Tripathi, 2015;
109 Chakraborty et al., 2015) as well. A Vaisala RH & T sensor was operated until the end of July
110 from which we have obtained RH & T values for the campaign. Wind speed and boundary layer
111 height data are obtained from NOAA ARL dataset. A 3 day (72 h) back trajectory cluster
112 analysis is carried out using HYSPLIT model with air masses arriving at every six hour interval
113 at a height of 500 m. This enabled us to understand the major directions from which the wind is
114 coming and possible impact of that.

115 Rainwater samples collector was placed on the rooftop (10 m above the ground and 1 m from the
116 floor of the roof) of the laboratory building inside which other instruments were housed.
117 Sampling was done manually on event basis using a wet collector, which was fitted with a 1-L
118 borosilicate glass made collecting flask (at the bottom) and polyethylene funnel 26 cm in
119 diameter. Before installation of collectors, the funnels and flasks were carefully cleaned (i.e.
120 soaked in 10% HNO₃ for many hours and rinsed several times with deionized water). During a
121 rain event, rainwater sample was collected after 30 min-1 h interval depending upon the rain
122 intensity, and a minimum of 50 ml rainwater was collected per rain event to make sure that
123 various kinds of analysis can be performed on these samples. Fog water samples were also
124 collected via Caltech 3 stage fog water collector for 2012-2015 winter (December-February)
125 period in 3 size fractions; coarse, medium and fine with 50% size cutoffs at 22, 16, 4 μ m,
126 respectively (Kaul et al., 2011; Raja et al., 2008). Immediately after collection, fog, and
127 rainwater samples were filtered through 0.22 μ m Whatman Nylon membrane filters to remove
128 suspended insoluble particles. Filtered samples were stored in pre-cleaned polypropylene bottle

129 in dark at -20°C until further analysis, which was completed within three weeks of the last
130 sample collection.

131 For analysis, filtered samples were then atomized using an atomizer (TSI Inc., USA) into the
132 AMS after passing through to a silica gel drier (outlet RH < 20%) to prevent clogging of
133 different instrument inlets and to avoid excessive moisture inside the AMS, which otherwise
134 complicates the use of standard fragmentation table. So, essentially in AMS we have analyzed
135 residues of fog and rain droplets, this may have resulted in loss of some small volatile organics
136 like formic acid, formaldehyde etc. However, those species are unlikely to remain in particle
137 phase under ambient conditions as well, so our inferences should still remain valid. This kind of
138 offline analysis with the help of an atomizer has been previously carried out throughout the
139 World (Joshi et al., 2012; Kaul et al., 2014; Lee et al., 2012) to understand different atmospheric
140 processes associated with cloud/fog water, filter extracts. Rain and fog water samples were also
141 analyzed for trace metals in Thermo Scientific ICP-OES (Inductively Coupled Plasma Optical
142 Emission Spectrometer, ICAP 6300 Thermo Inc.). This instrument uses superheated Argon
143 plasma of 7000–10000 K to break down and excite the atoms of the different elements and then
144 identifies the elements from the characteristic wavelength emitted during the excitation process.
145 It is a fairly rapid process and can identify up to 60 elements simultaneously. The instrument was
146 calibrated using a multi-element standard, and samples were blank corrected. Ten rainwater
147 samples were also analyzed in ion chromatography (Metrohm compact IC 761), for three anions
148 (Cl^- , NO_3^- , SO_4^{2-}). Details of IC and ICP-OES detection limit and methods can be found in
149 Chakraborty and Gupta, (2010).

150 **3. Results and discussion:**

151 **3.1 Composition and characteristics of ambient aerosols:**

152 AMS results reveal that monsoon time AA (Ambient aerosols) is dominated by organics as
153 observed for other seasons as well (winter, post monsoon) at this location (Bhattu and Tripathi,
154 2015; Chakraborty et al., 2015; Kaul et al., 2011). Sulfate is the second most dominant species in
155 AA followed by ammonium and nitrate (Fig. 1&2). Chloride is almost nonexistent during the
156 sampling period. Diurnal variations of different aerosol species (Fig. 2) revealed that all species
157 concentration peaked during the night, possibly due to lower boundary layer height, whereas
158 observed decrease during the afternoon was caused by boundary layer expansion and enhanced
159 mixing. Decrease in sulfate during the afternoon is relatively less pronounced, indicating that it is
160 simultaneously being produced via photochemistry. Sulfate and nitrate are completely
161 neutralized by ammonium which leads to non-acidic aerosols (Fig. 3) with ANR close to 1.

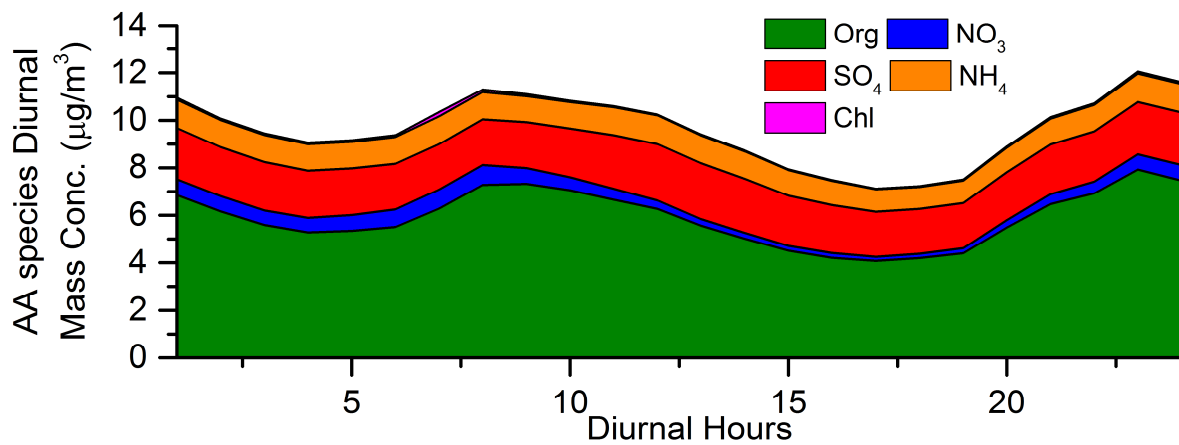
162 The aerosol neutralization ratio (ANR, equation 1) is defined in terms of the measured NH_4^+
163 (m)/ NH_4^+ (p) ratio (Chakraborty et al., 2015) as follows:
164 $\text{ANR} = \text{NH}_4^+ \text{measured (m)} / \text{NH}_4^+ \text{predicted (p)}$ ratio=

$$165 \frac{\text{NH}_4^+ \text{ (m)}}{18 \times \left(2 \times \frac{\text{SO}_4^{2-} \text{ (m)}}{96} + \frac{\text{NO}_3^- \text{ (m)}}{62} + \frac{\text{Cl}^- \text{ (m)}}{35.5} \right)} \quad (1)$$

166 where NH_4^+ (m), SO_4^{2-} (m), NO_3^- (m) and Cl^- (m) are the measured AMS mass concentrations of
167 ammonium, sulfate, nitrate, and chloride, respectively, and NH_4^+ (p) is the predicted mass
168 concentration of ammonium that was obtained by assuming that ammonium was the only cation
169 that balanced these anions.

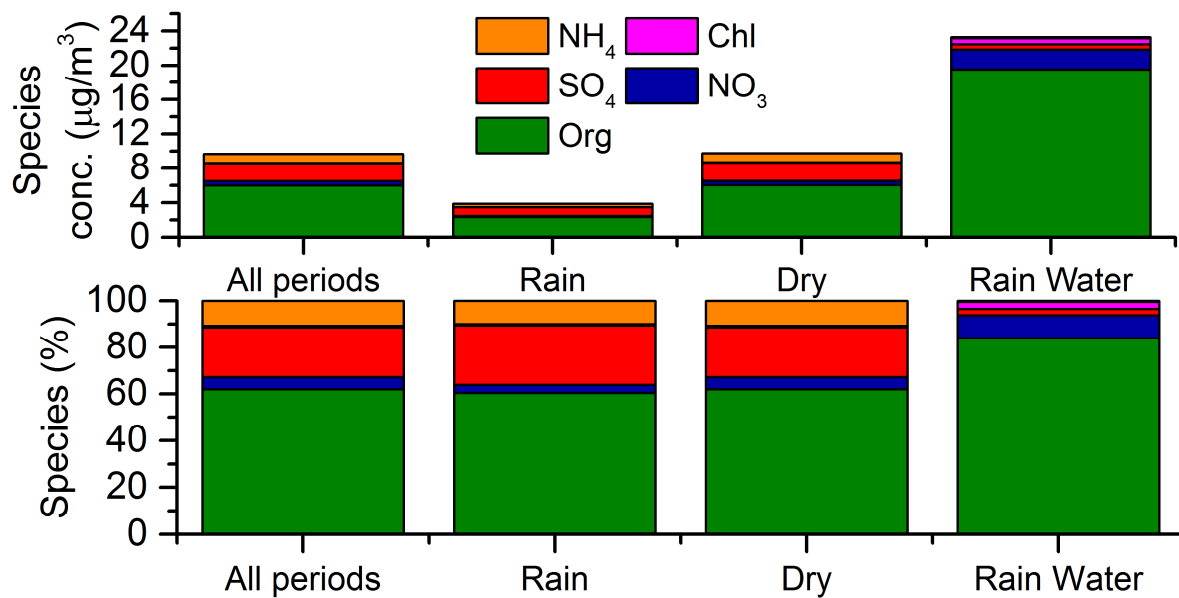
170 However, cation to anion ratio calculations in AMS can be misleading in case organo nitrates,
171 organo sulfates and/or sea/mineral salts are present in the aerosols. We found that $\text{NO}^+/\text{NO}_2^+$

172 ratio of AA (= 9.89) is much higher than the value obtained from IE calibrations with pure
173 NH_4NO_3 (= 3.5), indicating the presence of other forms of nitrate apart from NH_4NO_3 . Mineral
174 nitrate salts are usually associated with supermicron particles, and they have a very high
175 $\text{NO}^+/\text{NO}_2^+$ ratio (around 40), sea salt particles are also associated with larger particles
176 (Ovadnevaite et al., 2012) and have a very high $\text{NO}^+/\text{NO}_2^+$ ratio (Farmer et al., 2010). For the
177 present AMS, $\text{NO}^+/\text{NO}_2^+$ ratio for pure KNO_3 is 50, way above the observed ambient $\text{NO}^+/\text{NO}_2^+$
178 ratio of 9.89, indicating negligible contributions of sea salt/mineral nitrates to submicron AA.



179

180 Fig. 1: Diurnal profile of different NR-PM₁ species.

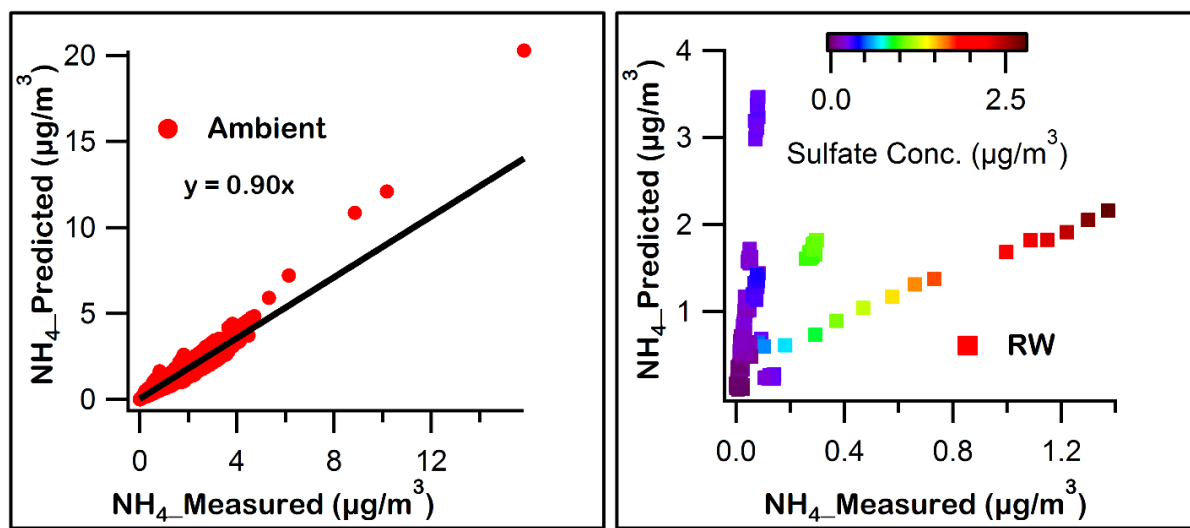


181

182 Fig. 2: Mass conc. and relative composition of NR-PM₁ aerosols present in ambient and
 183 rainwater (although rainwater concentrations may not be the representative of actual ambient
 184 concentrations as it is measured offline via atomization). “Rain” indicates PM₁ composition
 185 during rain events, while “dry” indicates PM₁ composition non rainy periods.

186 However, the observed NO⁺/NO₂⁺ ratio is very close to that reported for Organo nitrates (ON) in
 187 the literature (Farmer et al., 2010). Several organic nitrate fragments like; CH₄NO⁺, C₂H₅NO⁺,
 188 C₃H₄NO⁺ have also been observed in AMS HR mass spectra of AA, this confirms the presence
 189 of ON in AA. This also indicates that AA was probably alkaline in nature as AMS fragmentation
 190 table assign all nitrate fragments (NO⁺,NO₂⁺) to inorganic nitrate while some part of those
 191 fragments was actually originated from organic nitrates. This means that AMS is overestimating
 192 the inorganic nitrate and in spite of that, an ANR value close to 1 (Fig. 3) indicates that excess
 193 amount of ammonium is present in the ambient aerosols. However, some of this excess
 194 ammonium may be associated with organic acids which are not included in acidity calculations.
 195 This hypothesis is also supported by the positive correlation of f44 (AMS marker for organic

196 acids) with ANR (Fig. S1) and also reported in a filter study from this location (Singh and Gupta,
 197 2016). So, it's difficult to say conclusively whether AA was alkaline in nature or not, but higher
 198 pH values (range: 6.75-7.82) of rain water samples indicates that AA was most likely alkaline in
 199 nature. During rain events, overall composition changes only a little from dry time periods,
 200 however, the mass concentration of AA reduced significantly during these rain events (9.76 to
 201 3.88 $\mu\text{g}/\text{m}^3$, Fig. 2).



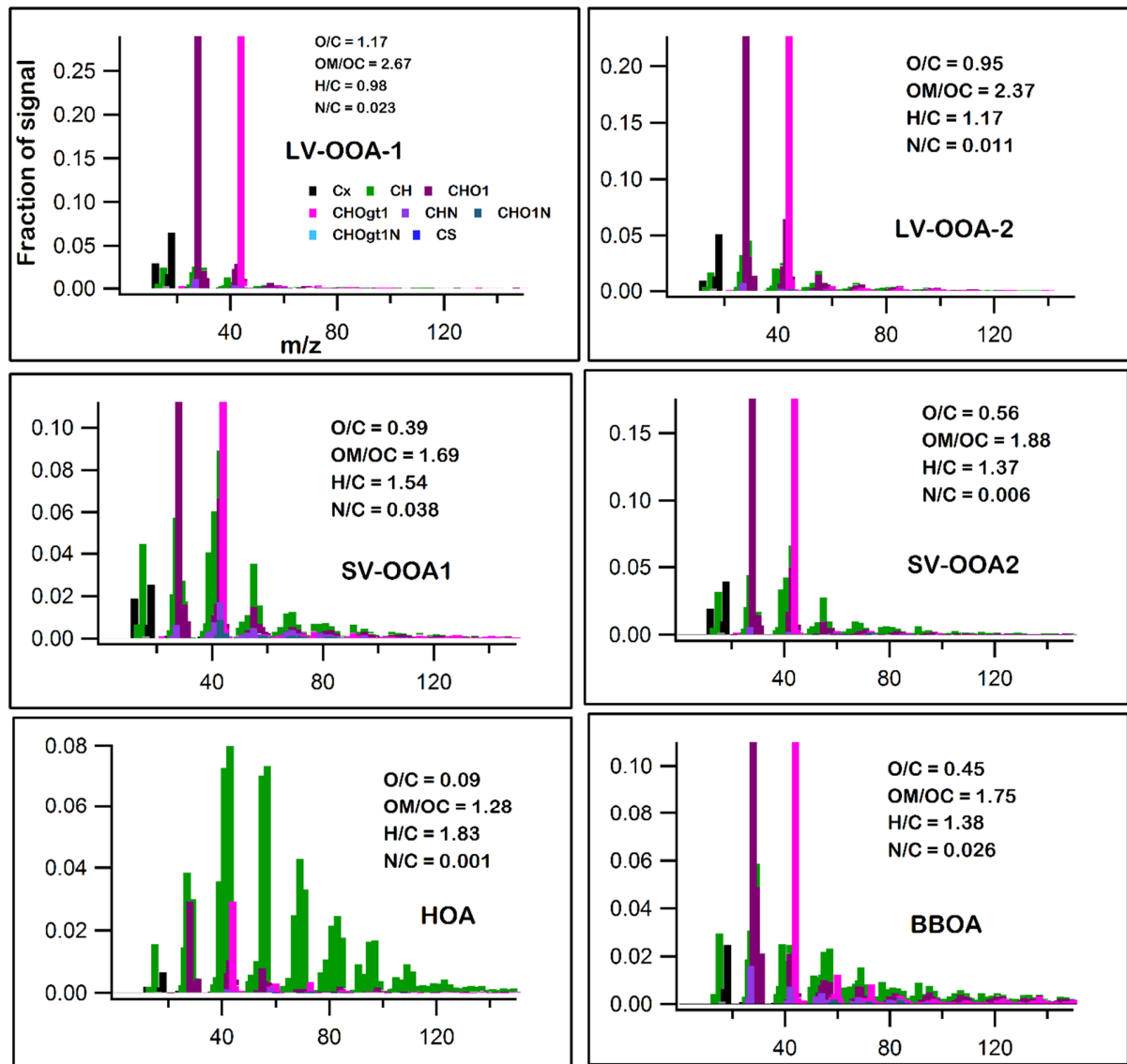
202 Fig. 3: Plot of AMS measured ammonium vs. required ammonium for neutralizing the anions.
 203 RW measured ammonium is way below the required value for complete neutralization.
 204 During rain events, AA (ANR = 0.87) are found to be slightly more acidic than dry periods
 205 (ANR = 1.04), mostly because of increased contribution from sulfate. Cloud processing is an
 206 important source of atmospheric sulfate (Moore et al., 2004; Raja et al., 2008), so it's possible
 207 that additional sulfate was produced inside the cloud and then came down with the precipitation,
 208 thus increasing its net concentration. No/little change in AA composition during rain events
 209 indicates that rain can equally efficiently remove all aerosols species. Sulfate showed a slight
 210 increase during the afternoon, indicating its photochemical production. Decrease in nitrate
 211 increase during the afternoon, indicating its photochemical production. Decrease in nitrate

212 concentration during daytime can be attributed to increased boundary layer height and higher
213 temperature which drives most of the particulate nitrate into gas phase.

214 **3.2 OA sources, composition, and characteristics:**

215 To gain further insight into the ambient OA composition and characteristics, source
216 apportionment via PMF (Paatero and Tapper, 1994; Ulbrich et al., 2009) is performed on the HR
217 organic mass spectra of AMS. PMF analysis is carried out with fpeak range of +5 to -5 with 0.5
218 increments and up to 12 factors. PMF factors are chosen based on their interpretability, PMF
219 diagnostics and factors correlation with external tracers (Fig. S2 & S3). The detailed rationale for
220 selecting the factors can be found in the supplementary information (SI). Three major types of
221 OA are identified, oxidized OA (OOA), Hydrocarbon like OA (HOA) and biomass burning OA
222 (BBOA). Chosen PMF solution has six factors (Fig. 4) but for diurnal variations and mass
223 concentrations, we have clubbed similar types of factors such as LV-OOA-1, 2 to LV-OOA and
224 SV-OOA1, 2 to SV-OOA thus reducing the number to 4 (Fig. S4). Time series of factors with
225 similar mass spectra and elemental ratios can be clubbed and presented as one factor, which can
226 make data representation much easier and has been followed in several studies (Docherty et al.,
227 2011; Timonen et al., 2013; Ulbrich et al., 2009). Detail description of these factors and their
228 diurnal variations can be found in supplementary (Section 1.1 and fig. S4).

229

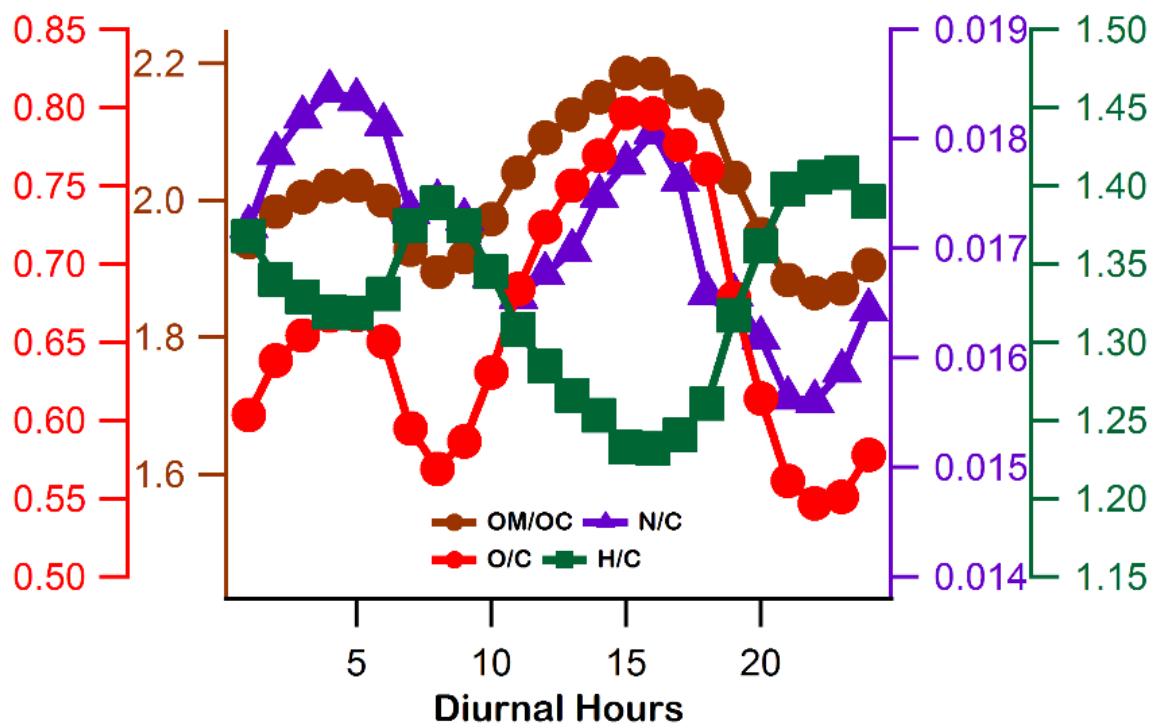


230

231 Fig. 4: Different types of OA, as identified by source apportionment of AMS ambient HR OA
 232 mass spectra via PMF.

233 Higher contributions from primary OAs (HO+BBOA) during early morning rush hours and night
 234 (Fig. S4) explains the significant diurnal variations in OA with peak concentration during those
 235 two periods (Fig. 1) of the day. Lower boundary layer height during those two time periods of
 236 the day may have also contributed to those observed peaks.

237 Elemental ratios of ambient OA also showed strong diurnal variations with O/C ratio peaking in
 238 the afternoon (Fig. 5) and dipping after sunset. Overall, daytime O/C ratio of 0.68 is much higher
 239 than night time O/C ratio of 0.58. Peaking of O/C ratio during afternoon coincides with the
 240 intense photochemistry and higher concentration of most oxidized LV-OOA (Fig. S4). Reduced
 241 O/C ratio during night time and early morning hours resulted from the absence of
 242 photochemistry with the higher concentration of primay OAs (HOA+BBOA) from traffic
 243 emissions and burning activities (Fig. S4).

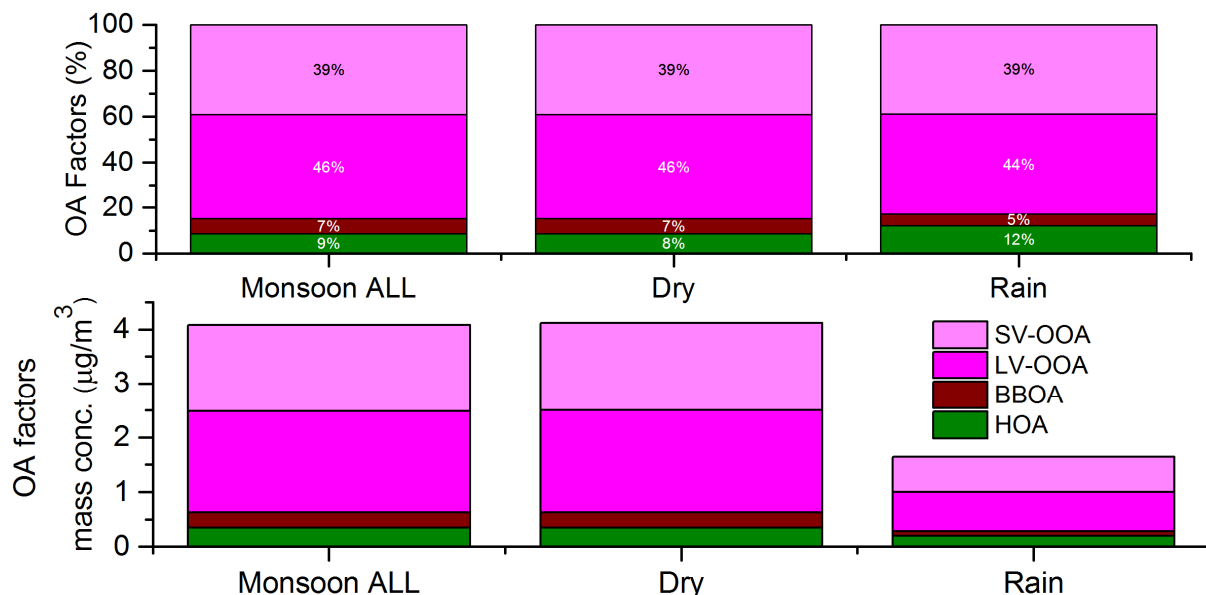


244

245 Fig. 5: Diurnal elemental ratios of ambient NR-PM₁. Daytime peak in O/C ratio clearly indicates
 246 production of oxidized OA via photochemistry.

247 OM/OC ratio followed the exactly similar trend as O/C ratio as expected while H/C ratio
 248 followed an opposite trend of O/C. Interestingly, during rain events, O/C of AA showed some
 249 reduction, from 0.67 during the dry period to 0.60 during rain events. This indicates that rain is

250 scavenging highly oxidized organics with a higher efficiency, possibly due to their higher
 251 polarity arising from higher oxygen content as reported for fog events from a previous study
 252 (Gilardoni et al., 2014). This is also evident from OA composition of monsoon time OA, which
 253 is completely dominated by oxidized OA (Fig. 6), with 85% mass of total ambient OA. Among
 254 oxidized OA, LV-OOA dominates over SV-OOA, indicating very high oxidation capacity of
 255 monsoon time ambient air and/or impact of long range transport as observed from the back
 256 trajectory analysis (Fig. S5). Among POAs, HOA dominates over BBOA, which is expected
 257 given that very low biomass burning activities are prevalent during monsoon time. During rain
 258 events, although OA mass decreased significantly by 60% (Fig. 6) overall OA composition
 259 remained the same (Fig. 6), indicating that rain droplets effectively scavenged all types OA.
 260 However, a slight enhancement in HOA contribution to ambient OA was observed during rain
 261 events (Fig. 6) which may indicate that efficiency of scavenging was slightly higher for other
 262 relatively more oxidized organics as compared to very less oxidized HOA.



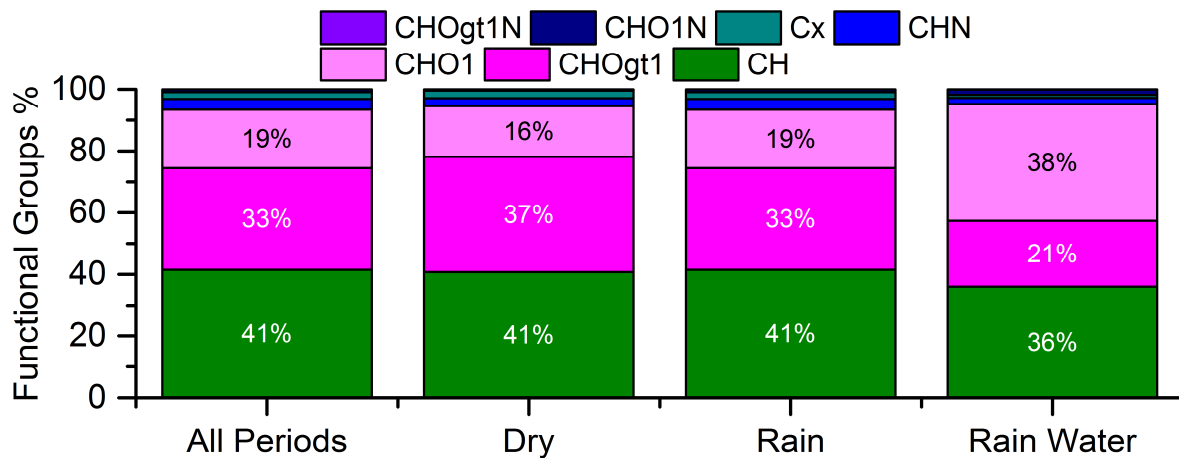
263

264 Fig. 6: Relative contributions of different types of OA to the total OA. Ambient OA is
265 overwhelmingly dominated by oxidized OA. Dry = non rainy periods.

266 Changes in OA elemental characteristics is examined via Van Krevelen (VK) diagram (H/C vs.
267 O/C plot), which shows that OA elemental ratios changes along a slope of -0.72 . Slopes of VK
268 diagram can sometimes be used to gain insight into OA aging mechanism, a relatively shallow
269 slope of -0.72 indicates the possible addition of $-\text{COOH}/-\text{OH}$ functional groups to the carbon
270 backbone (Heald et al., 2010; Ng et al., 2011). However, a particular slope or changes in slopes
271 of VK diagram can also be caused by mixing of different types of OA from various sources,
272 especially under ambient conditions. Thus, it's difficult to conclude whether the observed slope
273 is due to the addition of some particular functional groups, a particular type of oxidation
274 mechanism or due to mixing of different types of OA.

275 Ambient OA is dominated by oxidized organics fragments (aldehyde/acid/ketone etc.) as seen
276 from OA functional group composition in the AMS (Fig. 7). CHO1, CHOgt1 fragments (organic
277 fragments in AMS containing one and more than one oxygen, respectively) which are mostly
278 generated from carbonyls and organic acid compounds (Ng et al., 2011; Takegawa et al., 2009;
279 Zhang et al., 2007), contributes more than half of the ambient OA. CH fragments which mostly
280 comes from less oxidized hydrocarbon like organics (Ng et al., 2011; Takegawa et al., 2009),
281 contributes almost 40% to the total OA. However, OA functional group composition has
282 changed little from dry to rainy periods while O/C ratio has decreased substantially (0.67 to 0.60)
283 as mentioned earlier. These findings are at odds with each other; however, it is possible that
284 higher oxygen containing fragments of the CHOgt1 group have been removed more
285 preferentially during rain events thus leading to this substantial O/C ratio change but keeping
286 overall functional groups composition almost the same. A slight increase of less oxidized HOA

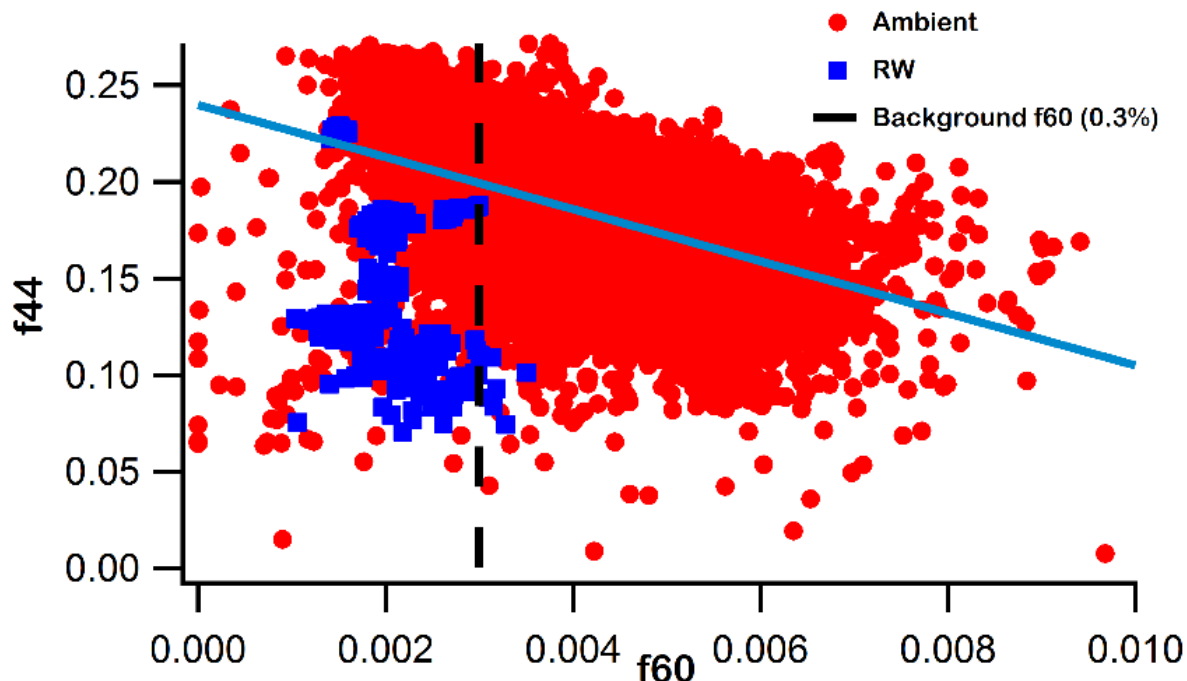
287 contribution and subsequent decrease in most oxidized LV-OOA contribution to total OA (Fig.
 288 6) during rain events can also explain this observed O/C decrease. During monsoon time,
 289 biomass burning activities in northern India are usually not very frequent or intense, which is
 290 also reflected in the PMF results with only 7% contribution from BBOA.



291
 292 Fig. 7: Contributions of different functional groups to total OA. Organics are dominated by
 293 oxidized functional groups under all circumstances.

294 Marker for biomass burning in AMS is m/z 60 or $C_2H_4O_2^+$, originates from levoglucosan
 295 fragmentation, its average relative contribution of 0.4% to total OA (m/z 60/total ambient OA or
 296 f_{60}) during the campaign period (Fig. 8) is very close to the typical background level f_{60} of
 297 0.3%, as mentioned in Cubison et al., (2011). This indicates that overall, a minor fraction of
 298 ambient OA originated from biomass burning activities during the campaign period. However,
 299 variations in f_{60} values are quite large, which means that some of the time periods were
 300 influenced by biomass burning activities and/or some other sources like coal combustion, which
 301 can also generate OA containing $C_2H_4O_2^+$ fragments (Wang et al., 2013). A strong anti-
 302 correlation is also observed between f_{60} and f_{44} (m/z 44/total OA), which indicates that primary

303 biomass burning OA (BBOA) are being oxidized to organic acids (as represented by f44 (Ng et
304 al., 2011; Takegawa et al., 2009)).



305

306 Fig. 8: Plot of f44 (a marker for carboxylic acids) vs. f60 (a marker for biomass burning). Strong
307 anti-correlation is observed for ambient OA while none is there for rainwater organics. In
308 rainwater f60 is below background level (0.3%), indicating that biomass burning OA may not be
309 very water soluble. Similar observations were also made during an aircraft based study at
310 Mexico City (Cubison et al., 2011).

311

312 **3.3 Comparison of monsoon time ambient OA composition with other seasons:**

313 Ambient OA loading and composition during monsoon time is very different from what was
314 observed during post monsoon and winter time (Bhattu and Tripathi, 2015; Chakraborty et al.,
315 2015) at this location. OA loading during monsoon (= 7.2 $\mu\text{g}/\text{m}^3$) is almost 10-15 times lower

316 than what was observed during post monsoon ($= 72 \mu\text{g}/\text{m}^3$, November 2012) and winter ($= 110$
317 $\mu\text{g}/\text{m}^3$, Dec 2012 – Jan 2013) (Chakraborty et al., 2015). Average O/C ratio during monsoon ($=$
318 0.65) is also higher than that observed for post monsoon and winter season ($= 0.50$ and 0.55 ,
319 respectively). This is not surprising as the dominance of oxidized OA in OA composition is
320 much more pronounced during monsoon than winter or post monsoon. During winter and post
321 monsoon oxidized OA contributed 57% and 69%, respectively to total OA, while during
322 monsoon that contribution is 85%, clearly indicating that during monsoon time OA was more
323 oxidized than other two seasons. However, during fog events O/C ratio of wintertime ambient
324 aerosols was increased by 15–20% while during rain events, O/C ratio of monsoon time AA was
325 decreased. This is possibly due to enhanced production of oxidized organics inside fog droplets
326 (Chakraborty et al., 2015; Ervens et al., 2011; Ge et al., 2012; Kaul et al., 2011) during fog
327 events which countered the removal of oxidized organics via fog scavenging and resulted in O/C
328 enhancement. Larger rain droplets can act more efficiently as a scavenger than smaller fog
329 droplets while due to their larger sizes, they have less residence time in ambient compared to
330 much smaller fog droplets. This possibly led to more scavenging and less aging/processing of
331 ambient aerosols. Apart from that, nature of aqueous processing and their end products may vary
332 significantly from more concentrated fog droplets to much diluted rain drops as reported for
333 cloud/fog droplets and aerosol water (Ervens et al., 2011).

334 Biomass burning contribution to OA was many times higher during the Nov-Jan period
335 compared to monsoon period. This is expected because of crop residue burning that takes place
336 every year during October – November (Bhattu and Tripathi, 2015) in Punjab and Haryana
337 (Northwestern part of India) and during winter, people in northern India burn several types of
338 biomass to get respite from cold (Behera and Sharma, 2010a; Kaul et al., 2011). So, huge

339 emissions of primary OA like BBOA, high OA loading and relatively weak solar radiation
340 during winter than monsoon have possibly caused this lower O/C ratio in winter compared to
341 monsoon. Also, unlike monsoon, no organo nitrates were identified in ambient aerosols during
342 those two seasons, indicating atmospheric processes may have been different during the
343 monsoon period.

344 **3.4 Analysis of rainwater residues composition:**

345 **3.4.1 Inorganics:**

346 Collected rainwater samples were analyzed in AMS. Each sample was atomized then passed
347 through the silica gel drier and then put into AMS for 30 minutes, and a few samples were
348 repeated twice to check reproducibility, which was excellent as every parameter was within 5%
349 of the original values during the duplicate run. Like AA, rainwater residues (RS) are also
350 dominated by organics and this dominance is even more pronounced in RS than AA (Fig. 2).
351 Unlike AA, instead of sulfate, nitrate is the second most dominant species in RS, followed by
352 sulfate and chloride. Ammonium concentration is almost negligible which led to ANR ratio of
353 0.11 for RS from AMS data, indicating that RS is extremely acidic. However, for the present
354 case, this ratio is very misleading as pH measurements of rainwater revealed it's mildly acidic to
355 alkaline nature with pH varying from 6.75-7.82. Apart from that concentration of alkali metals
356 like Ca, Mg, K, Na detected via ICP-OES is found to be sufficient for complete neutralization of
357 major anions (Cl^- , NO_3^- , SO_4^{2-}) detected via IC. Extremely low ANR for RS thus represents an
358 artifact of AMS measurement due to the presence of organo nitrates, organo sulfates and/or sea
359 salts like NaCl, KNO₃, and NaNO₃. The Very high average $\text{NO}^+/\text{NO}_2^+$ ratio of 14 (this value is
360 almost 40% higher than the observed value of 9.81 for AA) for RS is also an indication of that.
361 We have also detected very high concentrations of Na, K in RS from AMS data, much higher

362 than the values detected in AA, but part of these metals can also come from AMS vaporizer itself
363 (Canagaratna et al., 2007; DeCarlo et al., 2006). Although this makes quantification of Na and K
364 difficult in AMS, their relative trends can still be considered to gain insight into changes of K,
365 Na concentration in ambient air (Slowik et al., 2010). AMS measured Na^+ and chloride
366 concentrations in rainwater residues are highly correlated ($R^2 = 0.93$) while the correlation
367 between NH_4^+ and Cl^- is moderate ($R^2 = 0.50$). Also, correlation between AMS measured real-
368 time Na^+ and Cl^- is nonexistent ($R^2 = 0.02$) in AA, indicating that in RS, Na^+ is mostly in NaCl
369 form originating from sea salts. Sea salts are usually associated with larger super micron particle
370 sizes (Li et al., 2003; Murphy et al., 1998) and hence not detected during online sampling of AA
371 via AMS.

372 K^+ and Na^+ concentrations in RS are 15 & 17 times higher than the concentrations of these
373 elements found in AA. In RS, K^+ concentrations are on average ten times higher than K^+ in AA.
374 Also, K^+ concentrations are much higher than that NH_4^+ in RS, while the opposite is true for AA.
375 This suggests that a large part of the observed K^+ in RS originated from different sources as
376 compared to that present in AA. Since biomass burning activities were minimal during summer
377 monsoon and f60 levels are below background level in rainwater (Fig. 8), so another plausible
378 source of K is sea /mineral salt in the form of KNO_3 . Sea salt aerosols contain a high amount of
379 KCl , which can be converted to KNO_3 and K_2SO_4 during transport from source to receptor
380 location by interacting with nitrate & sulfate present in ambient air (Li et al., 2003; Song et al.,
381 2005). Correlations between K^+ , Na^+ , and NO_3^- are also much better than that of NH_4^+ and NO_3^-
382 (Fig. S6), indicating that in RS significant portion of nitrate may have come from $\text{KNO}_3/\text{NaNO}_3$.
383 However, in AA, no correlation is observed between AMS measured K^+ and NO_3^- ($R^2 = 0.01$),
384 indicating sources of nitrates were somewhat different for AA and RS. Also, with the inclusion

385 of AMS measured K⁺ and Na⁺ concentration as cations in rainwater ANR calculation, value
386 increased significantly to 0.72 from 0.11 (with NH₄⁺ as the only cation), indicating that most of
387 the anions are accounted for by these three cations. We have also identified some of the ON
388 fragments in AMS mass spectra of RS, similar to that of ambient OA. This indicates that some
389 ON is also present in rainwater OA as well, so it seems a combination of metallic and organo
390 nitrates resulted in such high NO⁺/NO₂⁺ ratio (= 14) for RS. Interestingly, the correlation
391 between NH₄⁺ and NO₃⁻ is slightly better for lower values of NH₄⁺, while the correlation of NH₄⁺
392 with SO₄²⁻, in general, is much stronger than with NO₃⁻. This indicates that higher values of
393 NH₄⁺ were associated mostly with SO₄²⁻ (Fig. 3).

394 **3.4.2 Elemental and sea salt contribution to rainwater residues**

395 Rainwater residues also contain several elements including some trace metals like Cu, Zn as
396 detected by ICP-OES. Among elements, Ca, Na, and K are 3 of the most abundant ones followed
397 by Mg, Zn, Mn, Cu & Ni (Fig. S7, 9). This finding also confirms that the AMS is capturing the
398 trends of Na⁺, K⁺ well as it also detected very high Na⁺ and K⁺ values. Other elements of Fe, Cr,
399 V, Pb were found to be below the detection limit of ICP-OES. The presence of K in spite of low
400 biomass burning activities indicates that it may have originated from sea salt. The abundance of
401 Na also indicates sea salt presence in the rainwater as observed in some other studies conducted
402 in Northern India (Satsangi et al., 1998; Tiwari et al., 2008, 2006), its strong correlation with K
403 indicates that both are being originated from similar sources. Zn present in the rainwater
404 residues may have come from tire wear, from tail pipes of the vehicles. Cu can also emit from
405 similar sources as Zn (Aatmeeeyata and Sharma, 2010; Aatmeeeyata et al., 2009). Ca usually found
406 in soil but there are some anthropogenic sources for it as well. To get an idea about possible
407 sources of these metals we have calculated their enrichment factors (EF).

408 EF = $(X/X_{ref})_{rainwater}/(X/X_{ref})_{crustal}$,

409 Where X = Element in question, X_{ref} = Reference element of predominantly crust origin (Mn for
410 this study)

411 EF are calculated using Ca as reference element as mentioned in several previous studies (Ghosh
412 et al., 2014; Loska et al., 2005, 2004). EF ~ 1, usually indicates crustal, non-anthropogenic
413 sources, while EF > 10 indicates a significant contribution from anthropogenic sources (Wang et
414 al., 2009, 2006). Calculated EF is highest for Zn followed by Cu, K, Na, and Mg. Only for Zn,
415 EF values are consistently above 10 in almost all the samples, indicating their anthropogenic
416 origins, while EF for Mg is consistently below one across the samples, indicating its crustal
417 origin (Fig. S7, 9). For K and Na, EF values are mostly below or slightly above 1 and matches
418 well with the values reported for marine aerosols by Weller et al., (2008), which means that they
419 mostly originated from natural sources (sea salt/crustal sources) with very low contributions
420 from anthropogenic emissions. In general, elements in smaller aerosols size fractions (PM₁,
421 PM_{2.5}) have much higher EF values compared to larger size fractions (PM₁₀, TSP) because of
422 higher anthropogenic contributions in finer fractions of PM. Therefore, much lower EF values of
423 different elements in rainwater residues support the hypothesis that rain droplets trapped mostly
424 larger, super micron size particles.

425 **3.4.3 Characteristics of rainwater organics:**

426 Relative contributions of different functional groups to residual rainwater organics (will be
427 referred to as residual OM from now onwards) are also different from that of ambient OA.
428 Although residual OM is also dominated by oxidized functional groups (CHO1, CHOgt1) like
429 ambient OA, this dominance is more pronounced in rainwater than ambient. Apart from that,

430 unlike ambient OA where CH functional group dominates, in rainwater organics, CHO1 group
431 fragments are the most abundant ones (Fig. 7). However, in the case of ambient OA, more
432 oxidized CHOgt1 fragments dominate over less oxidized CHO1 fragments, while the opposite is
433 true for residual OM, this has led to higher O/C ratio of ambient OA (O/C = 0.66) compared to
434 residual OM (O/C = 0.57). Observed O/C ratio of residual OM is also well within the range of
435 values (0.4 ± 0.3) reported for rain/cloud water organics via FT-ICR-MS in other studies (Mead
436 et al., 2013; Zhao et al., 2013). As in the case of ambient OA, residual OM also showed variation
437 in O/C ratios from day to night time samples of rainwater, with daytime O/C ratio of 0.59 is
438 found to be higher than the night time O/C ratio of 0.52. However, both day and night time O/C
439 ratios of residual OM are lower than the values observed for ambient OA (= 0.68 & 0.58,
440 respectively). Some of these differences between RS and AA can be explained by the fact that
441 rainwater can also scavenge and dissolve constituents of much larger particles than PM₁ very
442 efficiently (Croft et al., 2009; Henzing et al., 2006), which are mostly associated with mineral
443 dust, soil resuspension and sea spray with low organics content (Whitby and Cantrell, 1976).
444 However, in real time ambient sampling scenario AMS can only sample PM₁ dominated by
445 organics.

446 One interesting finding is the presence of organic sulfates in AMS HR mass spectra of residual
447 OM while none is found in ambient OA mass spectra. Organic sulfates can be present in the
448 atmosphere as sulfur adducts like; HMS (Hydroxymethanesulfaonate), MSA (Methanesulfonic
449 acid, $\text{CH}_3\text{SO}_3\text{H}$) or as separate organo sulfur (OS) compounds. Typical organic sulfur fragments
450 which are detected from AMS HR spectra in previously reported studies (Farmer et al., 2010; Ge
451 et al., 2012) includes; CH_2SO_2^+ , CH_3SO_2^+ , CH_2SO_3^+ and CHS, etc. Almost all of those fragments
452 are observed in collected RW samples (Fig. S8) confirming the presence of organo sulfur

453 compounds. These mainly originate from sulfur adducts to organic compounds like HMS, MSA.
454 Actual OS compounds usually get fragmented to SO^+ , SO_2^+ due to hard ionization of AMS.
455 However, if OS are present in sufficient quantity, then ratios like $\text{SO}^+/\text{SO}_3^+$, $\text{SO}_2^+/\text{SO}_3^+$ get
456 enhanced significantly as OS don't produce SO_3^+ fragments (Ge et al., 2012), so one can identify
457 qualitatively whether OS are present or not. For quantitative assessment, several OS standards
458 need to be run in the AMS, which unfortunately was not carried out in this study. Ge et al.,
459 (2012) developed an empirical method of calculating mass concentration of MSA from AMS
460 organo sulfur fragments like CH_2SO_2^+ , CH_3SO_2^+ and CH_4SO_3^+ , using that method we found that
461 MSA is contributing 9.5% of OOA (8% of total OA), which is much higher than 0.5% (of OOA)
462 reported by Ge et al., (2012) during foggy time, clearly indicating that here in RW, contributions
463 of organic sulfates are quite high. Hansen et al., (2015) recently shown from laboratory studies
464 that presence of organo sulfates can act as a very effective hygroscopic material and can reduce
465 the surface tension of a solution compared to pure water, especially in presence of inorganic salts
466 like ammonium sulfate. This indicates that organo sulfates can enhance the hygroscopicity of rain
467 water residues and they can more effectively work as condensation nuclei (CCN). In RS, almost
468 an order of magnitude enhancement in $\text{SO}^+/\text{SO}_3^+$, $\text{SO}_2^+/\text{SO}_3^+$ ratio (= 35 & 44, respectively) is
469 observed when compared to $\text{SO}^+/\text{SO}_3^+$, $\text{SO}_2^+/\text{SO}_3^+$ (= 6 & 7, respectively) ratio of pure
470 ammonium sulfate for the present AMS, which clearly indicates the presence of OS in rainwater.
471 Dissociation of dissolved metallic sulfates like K_2SO_4 , CaSO_4 can also alter this sulfate
472 fragmentation ratios. However, dissociation of metallic sulfates usually occurs at much higher
473 temperatures (Stern, 1974) than 600°C, so chances of their flash vaporization (within a few
474 seconds) at 600°C in AMS are very low (Drewnick et al., 2015). Some metallic sulfates can also
475 produce SO_3 fragment during decomposition which can actually bring down those above

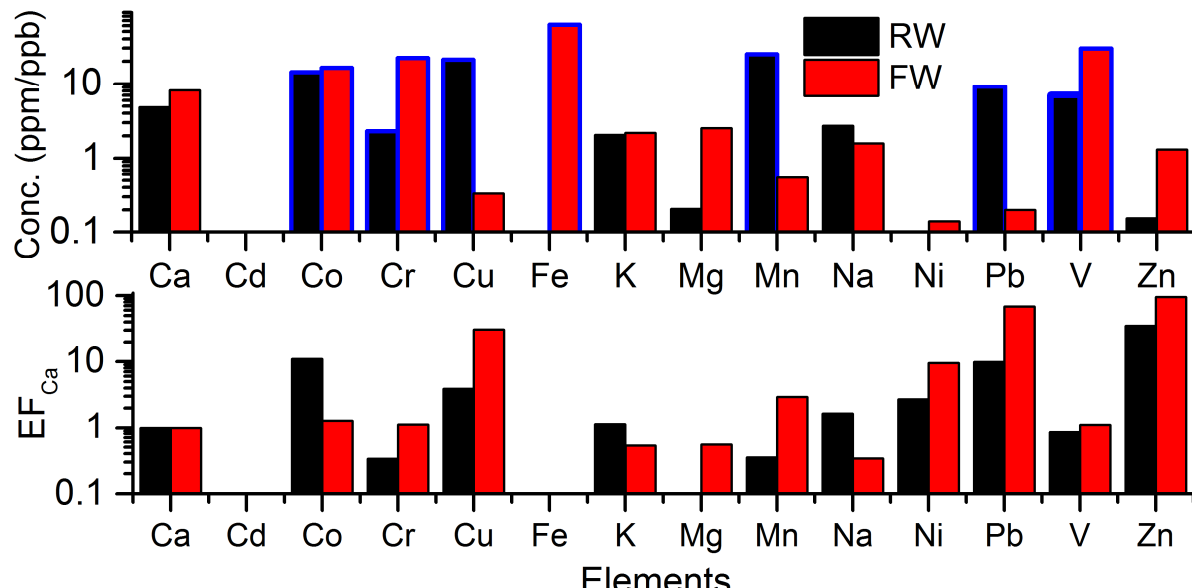
476 mentioned ratios. Apart from that $\text{SO}^+/\text{SO}_2^+$ ratio for RS and AA are close to each other ($= 0.68$
477 & 0.77 , respectively). These findings indicate that enhancement in $\text{SO}^+/\text{SO}_3^+$, $\text{SO}_2^+/\text{SO}_3^+$ ratios
478 are mainly due to the presence of OS.

479 The presence of OS is interesting as it considered to be a marker of aqueous processing and also
480 found in fog water samples (Dall’Osto et al., 2009; Ge et al., 2012). It’s possible that cloud
481 processing of organics and sulfur led to this formation of OS and sulfur adducts. However,
482 generally cloud processing led to the production of highly oxidized organics and enhancement of
483 O/C ratio (Ervens et al., 2011) but observed O/C ratio for residual OM is lower than ambient OA
484 as mentioned earlier. It is possible that larger, super micron particles, present in rainwater
485 contained less oxidized organics and given that 50-90% of the organics are found in submicron
486 particles (Hallquist et al., 2009; Ng et al., 2011) this finding is not surprising. The Larger
487 particles are also generally associated with mineral dust, soil resuspension and sea spray with
488 low organics content (Whitby and Cantrell, 1976). Another explanation could be underestimation
489 of oxygen content in OS and/or ON compounds by AMS, as their fragments like
490 NO^+ , NO_2^+ , SO^+ , SO_2^+ are typically treated as inorganics by standard AMS fragmentation table
491 (Allan, 2003; Farmer et al., 2010). As mentioned the earlier significant presence of OS
492 compounds detected in residual OM, so this may have led to O/C underestimation. In residual
493 OM, no anti correlation between f60 and f44 is observed (Fig. 8), in fact, f60 values are below
494 back ground levels ($< 0.3\%$) in residual OM, and this may indicate that organics from BB at this
495 location is not water soluble and/or it has been converted to some other oxidized form via
496 ambient oxidation processes (photochemistry/aqueous processing) (Cubison et al., 2011; Zhao et
497 al., 2014).

498 **3.4.4 Comparison of rain and fog water characteristics:**

499 Rain and fog both are natural cleansing agents but with very different characteristics like fog
500 droplets forms at ground level while rain droplets forms at an elevated level inside clouds. Rain
501 droplet sizes are usually much bigger and have much higher amount of LWC than fog droplets,
502 so it can more efficiently remove ambient aerosols. So, by comparing we are trying to
503 understand whether aerosol composition and chemistry are different within these two naturally
504 occurring aqueous medium. We will be comparing rainwater samples with coarser fog droplets
505 only as it has the largest droplet diameters ($> 22 \mu\text{m}$). Detailed analysis of size resolved fog
506 water (FW) samples are already reported as part of a submitted manuscript, so we will only be
507 discussing the major differences between coarse fog water and rainwater residues.
508 Concentrations of different species like elements, organics, sulfate, nitrate, ammonium, and
509 chloride are usually lower in rainwater residues than in fog water ones. This observation is
510 expected as fog droplets are much lower in size than rain droplets with less LWC (Beiderwieden
511 et al., 2005), so pollutants are more concentrated in them. Higher surface area of the smaller
512 droplets may have allowed them to dissolve more pollutants from surroundings. Apart from that
513 fog forms in the vicinity of the ground where pollutant concentrations are much higher than the
514 elevated altitudes where clouds are generally formed and lastly aerosol loadings during winter
515 were much higher than monsoon period. However, there are several differences in relative
516 composition and chemistry inside these two aqueous mediums which can't be explained only by
517 dilution or differences in aerosol loadings. For most of the anthropogenic elements, EF values
518 are higher in FW than in RS (Fig. 9), indicating that sources and nature of aerosols dissolved in
519 RS and FW may be very different.
520 Overall composition of both RS and FW are dominated by organics, but this domination is more
521 pronounced in RS than in FW. OM composition of RS is dominated by CHO1 functional groups

522 while that of FW is dominated by CH group, however in FW contribution of CHOgt1 functional
 523 group to total OA is much higher than that of in RS (Fig. S9). Also, f44 and O/C ratio (= 0.68) of
 524 FW are much higher than that of RS (= 0.58); this clearly indicates that FW is more processed
 525 and oxidized than RS (Fig. 10). Apart from that O/C ratio of FW (= 0.68) is much higher than
 526 that of winter time ambient aerosols (= 0.55) (Chakraborty et al., 2015), on the contrary, O/C
 527 ratio of RS (= 0.58) is lower than that of monsoon time ambient aerosols (= 0.67). These
 528 differences can't be explained by simple dilution or aerosol loadings differences as O/C; f44 are
 529 normalized parameters.

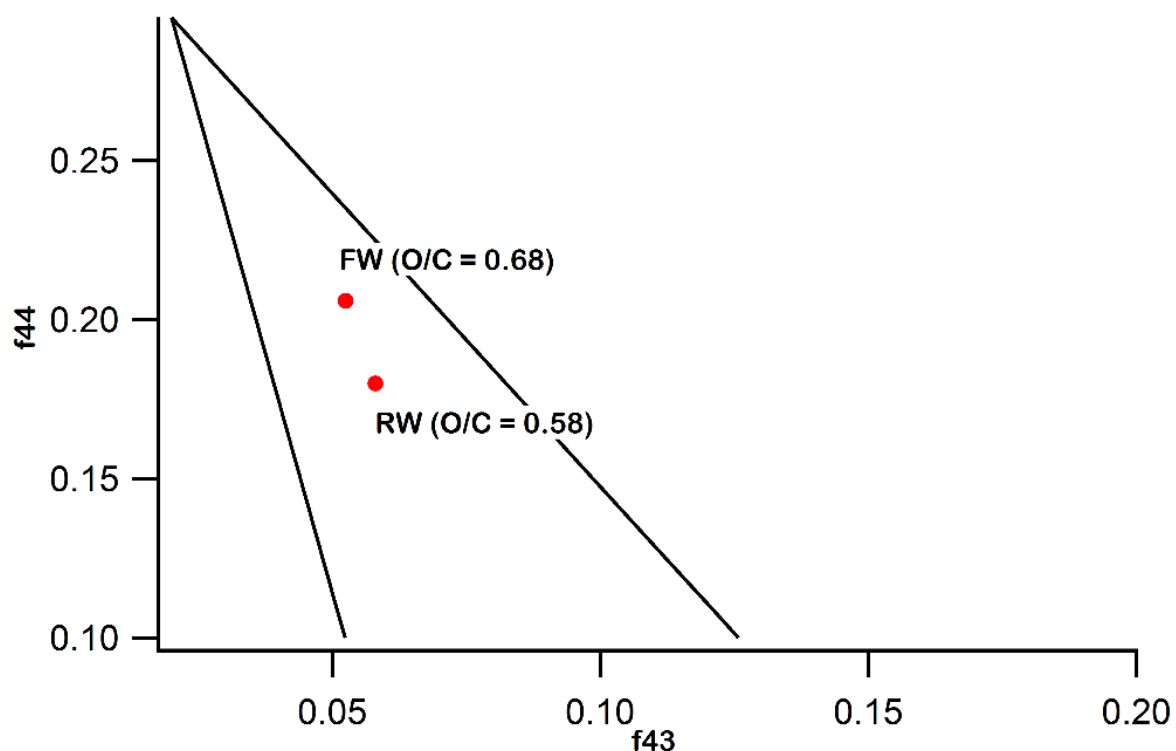


530

531 Fig. 9: Comparison of elemental concentrations and EF values between fog and rainwater
 532 samples. EF factor is calculated by taking Ca as a reference element. For blue bordered elements
 533 concentrations are in ppb while that of all others are in ppm.

534 However, several other factors can explain these differences; fog droplets being much smaller in
 535 size can remain in ambient for longer duration thus enhancing the processing time of dissolved
 536 aerosols. Due to smaller sizes, fog droplets can't capture much larger particles unlike rain

537 droplets, these larger particles may have been dominated by minerals and other species with very
538 little soluble organics or having less oxidized organics leading to this outcome. Relatively lower
539 EF values for dissolved elements in rainwater also suggests that aerosols trapped by rain droplets
540 are mostly originating from crustal sources/natural values. Apart from these differences, there are
541 some similarities like the dominance of organics and presence of organo sulfate in both RS and
542 FW, indicating some amount of aqueous processing is taking place within both the medium.



546 **4. Conclusions:**

547 Ambient and rainwater residues were analyzed by AMS in online and offline modes,
548 respectively. Both AA and RS are dominated by organics; this dominance is particularly

549 pronounced in RS. Inorganics are dominated by sulfate; however, enough ammonium is
550 available in the atmosphere to neutralize the anions completely. The presence of organic nitrate
551 is detected in AA via the elevated ratio of nitrate fragments ($\text{NO}^+/\text{NO}_2^+$). Source apportionment
552 of ambient OA indicates that ambient OA is comprised mostly of oxidized OA followed by
553 primary OA like biomass burning and hydrocarbon like OA. Contributions of oxidized OA to
554 total OA during monsoon is far higher than the same during post-monsoon and winter season,
555 indicating the higher oxidative capacity of atmosphere during monsoon. Although overall AA
556 composition remains the same, slight differences are observed in ambient OA composition from
557 rain events to dry periods. During rain events, the contribution of primary OA to ambient OA is
558 slightly increased along with a slight decrease in O/C ratio compared to dry periods. In RS, anion
559 concentrations are much higher than NH_4^+ concentrations, however considering other cations
560 like Na^+ and K^+ reduces this gap significantly, indicating a strong presence of other metallic salts
561 in rainwater. O/C ratio of rainwater organics are slightly lower than that of ambient OA, possibly
562 due to entrapment of metallic salts rich larger particle sizes with less oxidized organics. The
563 presence of organic sulfate and nitrates are detected in rainwater from HR AMS mass spectra.
564 This finding indicates that some aqueous processing inside the cloud may have taken place to
565 produce these organo sulfates, which are absent in ambient OA HR mass spectra. Comparison
566 with fog water samples revealed that RS is less oxidized and less concentrated possibly due to
567 the longer residence time of fog droplets and larger sizes of rain droplets. These findings indicate
568 that rainwater can effectively trap all types of aerosols including both oxidized and non-oxidized
569 organics, despite low hygroscopicity of the later. Monsoon time ambient aerosols are enriched
570 with oxidized organics which may promote the growth of cloud droplets due to their
571 hygroscopicity and higher oxygen content.

572

573 **Acknowledgements:**

574 We would like to acknowledge IIT Kanpur for providing us HR-ToF-AMS. We would also like
575 to NOAA ARL, for providing data of wind speed and boundary layer heights. We would also
576 like to acknowledge funds received from Indian National Science Academy to partially support
577 this study.

578

579

580

581

582

583

584

585

586

587

588

589

590

591

592

593

594

595

596

597

598 **References:**

599 Aatmeeyata, Kaul, D.S., Sharma, M., 2009. Traffic generated non-exhaust particulate emissions
600 from concrete pavement: A mass and particle size study for two-wheelers and small cars.
601 *Atmos. Environ.* 43, 5691–5697. doi:10.1016/j.atmosenv.2009.07.032

602 Aatmeeyata, Sharma, M., 2010. Polycyclic aromatic hydrocarbons, elemental and organic carbon
603 emissions from tire-wear. *Sci. Total Environ.* 408, 4563–4568.
604 doi:10.1016/j.scitotenv.2010.06.011

605 Allan, J.D., 2003. Quantitative sampling using an Aerodyne aerosol mass spectrometer: 2.
606 Measurements of fine particulate chemical composition in two U.K. cities. *J. Geophys. Res.*
607 108. doi:10.1029/2003JD001608

608 Behera, S.N., Sharma, M., 2010a. Reconstructing Primary and Secondary Components of PM2.5
609 Composition for an Urban Atmosphere. *Aerosol Sci. Technol.* 44, 983–992.
610 doi:10.1080/02786826.2010.504245

611 Behera, S.N., Sharma, M., 2010b. Investigating the potential role of ammonia in ion chemistry of
612 fine particulate matter formation for an urban environment. *Sci. Total Environ.* 408, 3569–
613 3575. doi:10.1016/j.scitotenv.2010.04.017

614 Beiderwieden, E., Wrzesinsky, T., Klemm, O., 2005. Chemical characterization of fog and rain
615 water collected at the eastern Andes cordillera. *Hydrol. Earth Syst. Sci.* 9, 185–191.
616 doi:10.5194/hessd-2-863-2005

617 Bhattu, D., Tripathi, S.N., 2015. CCN closure study: Effects of aerosol chemical composition
618 and mixing state. *J. Geophys. Res. Atmos.* 120, 766–783. doi:10.1002/2014JD021978

619 Cahill, C.F., Cahill, T.A., Perry, K.D., 2008. The size- and time-resolved composition of aerosols
620 from a sub-Arctic boreal forest prescribed burn. *Atmos. Environ.* 42, 7553–7559.
621 doi:10.1016/j.atmosenv.2008.04.034

622 Canagaratna, M.R., Jayne, J.T., Jimenez, J.L., Allan, J.D., Alfarra, M.R., Zhang, Q., Onasch,
623 T.B., Drewnick, F., Coe, H., Middlebrook, A., Delia, A., Williams, L.R., Trimborn, A.M.,
624 Northway, M.J., DeCarlo, P.F., Kolb, C.E., Davidovits, P., Worsnop, D.R., 2007. Chemical
625 and microphysical characterization of ambient aerosols with the aerodyne aerosol mass
626 spectrometer. *Mass Spectrom. Rev.* 26, 185–222. doi:10.1002/mas.20115

627 Carslaw, K.S., Lee, L.A., Reddington, C.L., Mann, G.W., Pringle, K.J., 2013. The magnitude
628 and sources of uncertainty in global aerosol. *Faraday Discuss.* 165, 495–512.
629 doi:10.1039/c3fd00043e

630 Chakraborty, A., Bhattu, D., Gupta, T., Tripathi, S.N., Canagaratna, M.R., 2015. Real-time
631 measurements of ambient aerosols in a polluted Indian city: Sources, characteristics and
632 processing of organic aerosols during foggy and non-foggy periods. *J. Geophys. Res.*
633 *Atmos.* 120, 9006–9019. doi:10.1002/2015JD023419

634 Chakraborty, A., Gupta, T., 2010. Chemical Characterization and Source Apportionment of
635 Submicron (PM1) Aerosol in Kanpur Region, India. *Aerosol Air Qual. Res.* 10, 433–445.
636 doi:10.4209/aaqr.2009.11.0071

637 Croft, B., Lohmann, U., Martin, R. V., Stier, P., Wurzler, S., Feichter, J., Posselt, R., Ferrachat,

638 S., 2009. Aerosol size-dependent below-cloud scavenging by rain and snow in the
639 ECHAM5-HAM. *Atmos. Chem. Phys.* 9, 4653–4675. doi:10.5194/acp-9-4653-2009

640 Cubison, M.J., Ortega, A.M., Hayes, P.L., Farmer, D.K., Day, D., Lechner, M.J., Brune, W.H.,
641 Apel, E., Diskin, G.S., Fisher, J.A., Fuelberg, H.E., Hecobian, A., Knapp, D.J., Mikoviny,
642 T., Riemer, D., Sachse, G.W., Sessions, W., Weber, R.J., Weinheimer, A.J., Wisthaler, A.,
643 Jimenez, J.L., 2011. Effects of aging on organic aerosol from open biomass burning smoke
644 in aircraft and laboratory studies. *Atmos. Chem. Phys.* 11, 12049–12064. doi:10.5194/acp-
645 11-12049-2011

646 Dall’Osto, M., Harrison, R.M., Coe, H., Williams, P., 2009. Real-time secondary aerosol
647 formation during a fog event in London. *Atmos. Chem. Phys.* 9, 2459–2469.
648 doi:10.5194/acp-9-2459-2009

649 DeCarlo, P.F., Kimmel, J.R., Trimborn, A., Northway, M.J., Jayne, J.T., Aiken, A.C., Gonin, M.,
650 Fuhrer, K., Horvath, T., Docherty, K.S., Worsnop, D.R., Jimenez, J.L., 2006. Field-
651 deployable, high-resolution, time-of-flight aerosol mass spectrometer. *Anal. Chem.* 78,
652 8281–8289. doi:10.1021/ac061249n

653 Docherty, K.S., Aiken, A.C., Huffman, J.A., Ulbrich, I.M., DeCarlo, P.F., Sueper, D., Worsnop,
654 D.R., Snyder, D.C., Peltier, R.E., Weber, R.J., Grover, B.D., Eatough, D.J., Williams, B.J.,
655 Goldstein, A.H., Ziemann, P.J., Jimenez, J.L., 2011. The 2005 Study of Organic Aerosols at
656 Riverside (SOAR-1): instrumental intercomparisons and fine particle composition. *Atmos.*
657 *Chem. Phys.* 11, 12387–12420. doi:10.5194/acp-11-12387-2011

658 Dockery, D.W., Pope, C. a, 1994. Acute respiratory effects of particulate air pollution. *Annu.*
659 *Rev. Public Health* 15, 107–132. doi:10.1146/annurev.pu.15.050194.000543

660 Drewnick, F., Diesch, J.-M., Faber, P., Borrmann, S., 2015. Aerosol mass spectrometry: particle-
661 vaporizer interactions and their consequences for the measurements. *Atmos. Meas. Tech.* 8,
662 3811–3830. doi:10.5194/amtd-8-3525-2015

663 Ervens, B., Turpin, B.J., Weber, R.J., 2011. Secondary organic aerosol formation in cloud
664 droplets and aqueous particles (aqSOA): a review of laboratory, field and model studies.
665 *Atmos. Chem. Phys.* 11, 11069–11102. doi:10.5194/acp-11-11069-2011

666 Farmer, D.K., Matsunaga, A., Docherty, K.S., Surratt, J.D., Seinfeld, J.H., Ziemann, P.J.,
667 Jimenez, J.L., 2010. Response of an aerosol mass spectrometer to organonitrates and
668 organosulfates and implications for atmospheric chemistry. *Proc. Natl. Acad. Sci. U. S. A.*
669 107, 6670–6675. doi:10.1073/pnas.0912340107

670 Ge, X., Zhang, Q., Sun, Y., Ruehl, C.R., Setyan, A., 2012. Effect of aqueous-phase processing
671 on aerosol chemistry and size distributions in Fresno, California, during wintertime.
672 *Environ. Chem.* 9, 221–235. doi:10.1071/en11168

673 Ghosh, S., Gupta, T., Rastogi, N., Gaur, A., Misra, A., Tripathi, S.N., Paul, D., Tare, V., Prakash,
674 O., Bhattu, D., Dwivedi, A.K., Kaul, D.S., Dalai, R., Mishra, S.K., 2014. Chemical
675 Characterization of Summertime Dust Events at Kanpur: Insight into the Sources and Level
676 of Mixing with Anthropogenic Emissions. *Aerosol Air Qual. Res.* 14, 879–891.
677 doi:10.4209/aaqr.2013.07.0240

678 Gilardoni, S., Massoli, P., Giulianelli, L., Rinaldi, M., Paglione, M., Pollini, F., Lanconelli, C.,

679 Poluzzi, V., Carbone, S., Hillamo, R., Russell, L.M., Facchini, M.C., Fuzzi, S., 2014. Fog
680 scavenging of organic and inorganic aerosol in the Po Valley. *Atmos. Chem. Phys.* 14,
681 6967–6981. doi:10.5194/acp-14-6967-2014

682 GOI, 2011. Indian Census 2011, Website: <http://www.census2011.co.in/census/district/535-kanpur-nagar.html>.

684 Hallquist, M., Wenger, J.C., Baltensperger, U., Rudich, Y., Simpson, D., Claeys, M., Dommen, J., Donahue, N.M., George, C., Goldstein, A.H., Hamilton, J.F., Herrmann, H., Hoffmann, T., Iinuma, Y., Jang, M., Jenkin, M.E., Jimenez, J.L., Kiendler-Scharr, A., Maenhaut, W., McFiggans, G., Mentel, T.F., Monod, A., Prevot, A.S.H., Seinfeld, J.H., Surratt, J.D., Szmigielski, R., Wildt, J., 2009. The formation, properties and impact of secondary organic aerosol: current and emerging issues. *Atmos. Chem. Phys.* 9, 5155–5236.

690 Hansen, A.M.K., Hong, J., Raatikainen, T., Kristensen, K., Ylisirniö, A., Virtanen, A., Petäjä, T., Glasius, M., Prisle, N.L., 2015. Hygroscopic properties and cloud condensation nuclei activation of limonene-derived organosulfates and their mixtures with ammonium sulfate. *Atmos. Chem. Phys.* 15, 14071–14089. doi:10.5194/acp-15-14071-2015

694 Heald, C.L., Kroll, J.H., Jimenez, J.L., Docherty, K.S., Decarlo, P.F., Aiken, a. C., Chen, Q., Martin, S.T., Farmer, D.K., Artaxo, P., 2010. A simplified description of the evolution of organic aerosol composition in the atmosphere. *Geophys. Res. Lett.* 37. doi:10.1029/2010GL042737.

698 Henzing, J.S., Olivié, D.J.L., Van Velthoven, P.F.J., 2006. A parameterization of size resolved below cloud scavenging of aerosols by rain. *Atmos. Chem. Phys. Discuss.* 6, 1355–1384. doi:10.5194/acpd-6-1355-2006

701 Hyvärinen, A.P., Raatikainen, T., Brus, D., Komppula, M., Panwar, T.S., Hooda, R.K., Sharma, V.P., Lihavainen, H., 2011. Effect of the summer monsoon on aerosols at two measurement stations in Northern India – Part 1: PM and BC concentrations. *Atmos. Chem. Phys.* doi:10.5194/acp-11-8271-2011

705 Hyvarinen, A.P., Raatikainen, T., Komppula, M., Mielonen, T., Sundstrom, A.M., Brus, D., Panwar, T.S., Hooda, R.K., Sharma, V.P., de Leeuw, G., Lihavainen, H., 2011. Effect of the summer monsoon on aerosols at two measurement stations in Northern India - Part 2: Physical and optical properties. *Atmos. Chem. Phys.* 11, 8283–8294. doi:DOI 10.5194/acp-11-8283-2011

710 Joshi, M., Sapra, B.K., Khan, A., Tripathi, S.N., Shamjad, P.M., Gupta, T., Mayya, Y.S., 2012. Harmonisation of nanoparticle concentration measurements using GRIMM and TSI scanning mobility particle sizers. *J. Nanoparticle Res.* 14. doi:10.1007/s11051-012-1268-8

713 Kaul, D.S., Gupta, T., Tripathi, S.N., 2014. Source Apportionment for Water Soluble Organic Matter of Submicron Aerosol: A Comparison between Foggy and Nonfoggy Episodes. *Aerosol Air Qual. Res.* 14, 1527 – 1533. doi:10.4209/aaqr.2013.10.0319

716 Kaul, D.S., Gupta, T., Tripathi, S.N., Tare, V., Collett Jr., J.L., 2011. Secondary Organic Aerosol: A Comparison between Foggy and Nonfoggy Days. *Environ. Sci. Technol.* 45, 7307–7313. doi:10.1021/es201081d

719 Khare, P., Kumar, N., Satsangi, G.S., Kumari, K.M., Srivastava, S.S., 1998. Formate and acetate

720 in particulate matter and dust pall at Dayalbagh, Agra (India). *Chemosphere* 36, 2993–3002.
721 doi:10.1016/S0045-6535(97)10096-0

722 Khare, P., Satsangi, G.S., Kumar, N., Kumari, K.M., Srivastava, S.S., 1997. HCHO, HCOOH
723 and CH₃COOH in air and rain water at a rural tropical site in north central India. *Atmos.*
724 *Environ.* 31, 3867–3875. doi:10.1016/S1352-2310(97)00263-X

725 Kulshreshta, U., Kumar, N., Saxena, A., 1993. Effect of anthropogenic activity on formate and
726 acetate levels in precipitation at four sites in Agra, India. *Atmos. Environ. Part B.* 27B, 87–
727 91.

728 Kulshrestha, U.C., Granat, L., Engardt, M., Rodhe, H., 2005. Review of precipitation monitoring
729 studies in India - A search for regional patterns. *Atmos. Environ.* 39, 7403–7419.
730 doi:10.1016/j.atmosenv.2005.08.035

731 Lee, A.K.Y., Hayden, K.L., Herckes, P., Leaitch, W.R., Liggio, J., Macdonald, A.M., Abbatt,
732 J.P.D., 2012. Characterization of aerosol and cloud water at a mountain site during WACS
733 2010: secondary organic aerosol formation through oxidative cloud processing. *Atmos.*
734 *Chem. Phys.* 12, 7103–7116. doi:10.5194/acp-12-7103-2012

735 Lelieveld, J., Crutzen, P.J., Ramanathan, V., Andreae, M.O., Brenninkmeijer, C.M., Campos, T.,
736 Cass, G.R., Dickerson, R.R., Fischer, H., de Gouw, J. a, Hansel, A., Jefferson, A., Kley, D.,
737 de Laat, a T., Lal, S., Lawrence, M.G., Lobert, J.M., Mayol-Bracero, O.L., Mitra, a P.,
738 Novakov, T., Oltmans, S.J., Prather, K. a, Reiner, T., Rodhe, H., Scheeren, H. a, Sikka, D.,
739 Williams, J., 2001. Pollution from South and Southeast Asia The Indian Ocean Experiment :
740 Widespread Air Pollution from South and Southeast Asia. *Science* (80-). 291, 1031–1036.
741 doi:10.1126/science.1057103

742 Li, J., Pósfai, M., Hobbs, P. ~V. P. V., Buseck, P. ~R. P.R., Posfai, M., Hobbs, P. ~V. P. V.,
743 Buseck, P. ~R. P.R., 2003. Individual Aerosol Particles from Biomass Burning in Southern
744 Africa Compositions and Aging of Inorganic Particles. *J. Geophys. Res.* 108, 1–12.
745 doi:10.1029/2002JD002310

746 Loska, K., Wiechuła, D., Pelczar, J., 2005. Application of Enrichment Factor to Assessment of
747 Zinc Enrichment/Depletion in Farming Soils. *Commun. Soil Sci. Plant Anal.* 36, 1117–
748 1128. doi:10.1081/CSS-200056880

749 Loska, K., Wiechuła, D., Korus, I., 2004. Metal contamination of farming soils affected by
750 industry. *Environ. Int.* 30, 159–165. doi:10.1016/S0160-4120(03)00157-0

751 Malik, A., Singh, V.K., Singh, K.P., 2007. Occurrence and distribution of persistent trace
752 organics in rainwater in an urban region (India). *Bull. Environ. Contam. Toxicol.* 79, 639–
753 645. doi:10.1007/s00128-007-9290-8

754 Mead, R.N., Mullaugh, K.M., Brooks Avery, G., Kieber, R.J., Willey, J.D., Podgorski, D.C.,
755 2013. Insights into dissolved organic matter complexity in rainwater from continental and
756 coastal storms by ultrahigh resolution Fourier transform ion cyclotron resonance mass
757 spectrometry. *Atmos. Chem. Phys.* 13, 4829–4838. doi:10.5194/acp-13-4829-2013

758 Middlebrook, A.M., Bahreini, R., Jimenez, J.L., Canagaratna, M.R., 2012. Evaluation of
759 Composition-Dependent Collection Efficiencies for the Aerodyne Aerosol Mass
760 Spectrometer using Field Data. *Aerosol Sci. Technol.* 46, 258–271.

761 doi:10.1080/02786826.2011.620041

762 Mishra, S.K., Dey, S., Tripathi, S.N., 2008. Implications of particle composition and shape to
763 dust radiative effect: A case study from the Great Indian Desert. *Geophys. Res. Lett.* 35, 1–
764 5 (L23814). doi:10.1029/2008GL036058

765 Misra, A., Gaur, A., Bhattu, D., Ghosh, S., Dwivedi, A.K., Dalai, R., Paul, D., Gupta, T., Tare,
766 V., Mishra, S.K., Singh, S., Tripathi, S.N., 2014. An overview of the physico-chemical
767 characteristics of dust at Kanpur in the central Indo-Gangetic basin. *Atmos. Environ.* 97,
768 386–396. doi:10.1016/j.atmosenv.2014.08.043

769 Moore, K.F., Sherman, D.E., Reilly, J.E., Collett, J.L., 2004. Drop size-dependent chemical
770 composition in clouds and fogs. Part I. Observations. *Atmos. Environ.* 38, 1389–1402.
771 doi:10.1016/j.atmosenv.2003.12.013

772 Murphy, D.M., Anderson, J.R., Quinn, P.K., McInnes, L.M., Brechtel, F.J., Kreidenweis, S.M.,
773 Middlebrook, a. M., P[acute]sfai, M., Thomson, D.S., Buseck, P.R., 1998. Influence of
774 sea-salt on aerosol radiative properties in the Southern Ocean marine boundary layer.
775 *Nature* 392, 62–65. doi:10.1038/32138

776 Nakajima, T., Yoon, S.C., Ramanathan, V., Shi, G.Y., Takemura, T., Higurashi, A., Takamura,
777 T., Aoki, K., Sohn, B.J., Kim, S.W., Tsuruta, H., Sugimoto, N., Shimizu, A., Tanimoto, H.,
778 Sawa, Y., Lin, N.H., Lee, C. Te, Goto, D., Schutgens, N., 2007. Overview of the
779 Atmospheric Brown Cloud East Asian Regional Experiment 2005 and a study of the aerosol
780 direct radiative forcing in east Asia. *J. Geophys. Res. Atmos.* 112, 1–23.
781 doi:10.1029/2007JD009009

782 National ambient air quality standards, 2012. National ambient air quality status & trends in
783 india-2010 central pollution control board. GOI.

784 Ng, N.L., Canagaratna, M.R., Jimenez, J.L., Chhabra, P.S., Seinfeld, J.H., Worsnop, D.R., 2011.
785 Changes in organic aerosol composition with aging inferred from aerosol mass spectra.
786 Atmos. Chem. Phys. 11, 6465–6474. doi:10.5194/acp-11-6465-2011

787 Norris, G., Larson, T., Koenig, J., Claiborn, C., Sheppard, L., Finn, D., 2000. Asthma
788 aggravation, combustion, and stagnant air. *Thorax* 55, 466–470.
789 doi:10.1136/thorax.55.6.466

790 Ovadnevaite, J., Ceburnis, D., Canagaratna, M., Berresheim, H., Bialek, J., Martucci, G.,
791 Worsnop, D.R., O'Dowd, C., 2012. On the effect of wind speed on submicron sea salt mass
792 concentrations and source fluxes. *J. Geophys. Res.* 117. doi:10.1029/2011jd017379

793 Paatero, P., Tapper, U., 1994. Positive Matrix Factorization - A Nonnegative Factor Model with
794 Optimal Utilization of Error Estimates of Data Values. Environmetrics 5, 111–126.
795 doi:10.1002/env.3170050203

796 Raja, S., Raghunathan, R., Yu, X.-Y., Lee, T., Chen, J., Kommalapati, R.R., Murugesan, K.,
797 Shen, X., Qingzhong, Y., Valsaraj, K.T., Collett Jr., J.L., 2008. Fog chemistry in the Texas-
798 Louisiana Gulf Coast corridor. *Atmos. Environ.* 42, 2048–2061.
799 doi:10.1016/j.atmosenv.2007.12.004

800 Ramanathan, V., Li, F., Ramana, M. V., Praveen, P.S., Kim, D., Corrigan, C.E., Nguyen, H.,

801 Stone, E. a., Schauer, J.J., Carmichael, G.R., Adhikary, B., Yoon, S.C., 2007. Atmospheric
802 brown clouds: Hemispherical and regional variations in long-range transport, absorption,
803 and radiative forcing. *J. Geophys. Res. Atmos.* 112, 1–26. doi:10.1029/2006JD008124

804 Salve, P.R., Lohkare, H., Gobre, T., Bodhe, G., Krupadom, R.J., Ramteke, D.S., Wate, S.R.,
805 2012. Characterization of chromophoric dissolved organic matter (CDOM) in rainwater
806 using fluorescence spectrophotometry. *Bull. Environ. Contam. Toxicol.* 88, 215–218.
807 doi:10.1007/s00128-011-0424-7

808 Satsangi, G.S., Lakhani, a., Khare, P., Singh, S.P., Kumari, K.M., Srivastava, S.S., 1998.
809 Composition of rain water at a semi-arid rural site in India. *Atmos. Environ.* 32, 3783–3793.
810 doi:10.1016/S1352-2310(98)00115-0

811 Singh, D.K., Gupta, T., 2016. Role of transition metals with water soluble organic carbon in the
812 formation of secondary organic aerosol and metallo-organics in PM1 sampled during post
813 monsoon and pre-winter time. *J. Aerosol Sci.* 94, 56–69. doi:10.1016/j.jaerosci.2016.01.002

814 Slowik, J.G., Stroud, C., Bottenheim, J.W., Brickell, P.C., Chang, R.Y.-W., Liggio, J., Makar,
815 P.A., Martin, R. V., Moran, M.D., Shantz, N.C., Sjostedt, S.J., van Donkelaar, A.,
816 Vlasenko, A., Wiebe, H.A., Xia, A.G., Zhang, J., Leaitch, W.R., Abbatt, J.P.D., 2010.
817 Characterization of a large biogenic secondary organic aerosol event from eastern Canadian
818 forests. *Atmos. Chem. Phys.* 10, 2825–2845. doi:10.5194/acpd-9-18113-2009

819 Song, C.H., Ma, Y., Orsini, D., Kim, Y.P., Weber, R.J., 2005. An investigation into the ionic
820 chemical composition and mixing state of biomass burning particles recorded during
821 TRACE-P P3B Flight#10. *J. Atmos. Chem.* 51, 43–64. doi:10.1007/s10874-005-5727-9

822 Stern, K.H., 1974. High Temperature Properties and Decomposition of Inorganic Salts with
823 Oxyanions. *J. Phys. Chem. Ref. Data* 3, 481. doi:10.1063/1.3253144

824 Takegawa, N., Miyakawa, T., Watanabe, M., Kondo, Y., Miyazaki, Y., Han, S., Zhao, Y., van
825 Pinxteren, D., Bruggemann, E., Gnauk, T., Herrmann, H., Xiao, R., Deng, Z., Hu, M., Zhu,
826 T., Zhang, Y., 2009. Performance of an Aerodyne Aerosol Mass Spectrometer (AMS)
827 during Intensive Campaigns in China in the Summer of 2006. *Aerosol Sci. Technol.* 43,
828 189–204. doi:10.1080/02786820802582251

829 Timonen, H., Carbone, S., Aurela, M., Saarnio, K., Saarikoski, S., Ng, N.L., Canagaratna, M.R.,
830 Kulmala, M., Kerminen, V.-M., Worsnop, D.R., Hillamo, R., 2013. Characteristics, sources
831 and water-solubility of ambient submicron organic aerosol in springtime in Helsinki,
832 Finland. *J. Aerosol Sci.* 56, 61–77. doi:10.1016/j.jaerosci.2012.06.005

833 Tiwari, S., Ranade, A., Singh, D., Pandey, A.K., 2006. Study of chemical species in rainwater at
834 Ballia, a rural environment in eastern Uttar Pradesh, India. *Indian J. Radio Sp. Phys.* 35, 35–
835 41.

836 Tiwari, S., Srivastava, M.K., Bisht, D.S., 2008. Chemical composition of rainwater in Panipat ,
837 an industrial city in Haryana. *Indian J. Radio Sp. Phys.* 37, 443–449.

838 Ulbrich, I.M., Canagaratna, M.R., Zhang, Q., Worsnop, D.R., Jimenez, J.L., 2009. Interpretation
839 of organic components from Positive Matrix Factorization of aerosol mass spectrometric
840 data. *Atmos. Chem. Phys.* 9, 2891–2918.

841 Wang, G., Kawamura, K., Lee, M., 2009. Comparison of organic compositions in dust storm and
842 normal aerosol samples collected at Gosan, Jeju Island, during spring 2005. *Atmos.*
843 *Environ.* 43, 219–227. doi:10.1016/j.atmosenv.2008.09.046

844 Wang, X., Williams, B.J., Tang, Y., Huang, Y., Kong, L., Yang, X., Biswas, P., 2013.
845 Characterization of organic aerosol produced during pulverized coal combustion in a drop
846 tube furnace. *Atmos. Chem. Phys.* 13, 10919–10932. doi:10.5194/acp-13-10919-2013

847 Wang, Y., Zhuang, G., Zhang, X., Huang, K., Xu, C., Tang, A., Chen, J., An, Z., 2006. The ion
848 chemistry, seasonal cycle, and sources of PM_{2.5} and TSP aerosol in Shanghai. *Atmos.*
849 *Environ.* 40, 2935–2952. doi:10.1016/j.atmosenv.2005.12.051

850 Weller, R., Wöltjen, J., Piel, C., Resenbergs, R., Wagenbach, D., König-Langlo, G., Kriewa, M.,
851 2008. Seasonal variability of crustal and marine trace elements in the aerosol at Neumayer
852 station, Antarctica. *Tellus B* 60, 742–752. doi:10.1111/j.1600-0889.2008.00372.x

853 Whitby, K.T., Cantrell, B., 1976. Atmospheric aerosols- Characteristics and measurement, in:
854 International Conference on Environmental Sensing and Assessment, Las Vegas, Nev. p. 1.

855 Yadav, S., Tandon, A., Attri, A.K., 2013. Characterization of aerosol associated non-polar
856 organic compounds using TD-GC-MS: A four year study from Delhi, India. *J. Hazard.*
857 *Mater.* 252, 29–44. doi:10.1016/j.jhazmat.2013.02.024

858 Zhang, Q., Jimenez, J.L., Canagaratna, M.R., Allan, J.D., Coe, H., Ulbrich, I., Alfarra, M.R.,
859 Takami, A., Middlebrook, A.M., Sun, Y.L., Dzepina, K., Dunlea, E., Docherty, K.,
860 DeCarlo, P.F., Salcedo, D., Onasch, T., Jayne, J.T., Miyoshi, T., Shimono, A., Hatakeyama, S.,
861 Takegawa, N., Kondo, Y., Schneider, J., Drewnick, F., Borrmann, S., Weimer, S.,
862 Demerjian, K., Williams, P., Bower, K., Bahreini, R., Cottrell, L., Griffin, R.J., Rautiainen, J.,
863 Sun, J.Y., Zhang, Y.M., Worsnop, D.R., 2007. Ubiquity and dominance of oxygenated
864 species in organic aerosols in anthropogenically-influenced Northern Hemisphere
865 midlatitudes. *Geophys. Res. Lett.* 34. doi:10.1029/2007gl029979

866 Zhao, R., Mungall, E.L., Lee, A.K.Y., Aljawhary, D., Abbatt, J.P.D., 2014. Aqueous-phase
867 photooxidation of levoglucosan – a mechanistic study using aerosol time-of-flight
868 chemical ionization mass spectrometry (Aerosol ToF-CIMS). *Atmos. Chem. Phys.* 14,
869 9695–9706. doi:10.5194/acp-14-9695-2014

870 Zhao, Y., Hallar, A.G., Mazzoleni, L.R., 2013. Atmospheric organic matter in clouds: exact
871 masses and molecular formula identification using ultrahigh-resolution FT-ICR mass
872 spectrometry. *Atmos. Chem. Phys.* 13, 12343–12362. doi:10.5194/acp-13-12343-2013

873